

Metallurgy and Foundry Engineering – Vol. 43, 2017, No. 1, pp. 67–72
<http://dx.doi.org/10.7494/mafe.2017.43.1.67>

Mirosława Wojciechowska, Krzysztof Ziewiec, Jarosław Ferenc

Investigations of microstructure and phase transformations of $\text{Fe}_{71,25}\text{Si}_{9,5}\text{B}_{14,25}\text{In}_5$ alloy

Badania mikrostruktury i przemian fazowych w stopie $\text{Fe}_{71,25}\text{Si}_{9,5}\text{B}_{14,25}\text{In}_5$

Abstract

The aim of this work was to study the microstructure and high-temperature phase transformations of the $\text{Fe}_{71,25}\text{Si}_{9,5}\text{B}_{14,25}\text{In}_5$ alloy. The alloy was remelted in a resistance furnace, and a sequence of melting and crystallization at a range of high temperatures was observed using a mid-wave infrared MWIR camera. The alloy was also investigated by differential thermal analysis (DTA). The microstructure of the alloy was studied using a scanning electron microscope SEM with an energy dispersive spectrometer (EDS). The results show that there is a clear partition into two liquids in the studied alloy. The ingot microstructure presents very strong segregation into the eutectic regions enriched in the Fe-Si-B and In-rich regions.

Keywords: amorphous/crystalline composite, mid-wave infrared camera, scanning electron microscope (SEM), differential thermal analysis (DTA)

Streszczenie

Celem pracy było zbadanie mikrostruktury oraz wysokotemperaturowych przemian fazowych zachodzących w stopie $\text{Fe}_{71,25}\text{Si}_{9,5}\text{B}_{14,25}\text{In}_5$. Proces przetapiania oraz krystalizacji stopu w piecu oporowym został zarejestrowany za pomocą kamery termowizyjnej pracującej w zakresie średniofalowej podczerwieni. Wykonano również różnicową analizę termiczną DTA badanego stopu. Mikrostrukturę zbadano przy użyciu skaningowego mikroskopu elektronowego SEM wyposażonego w spektrometr energii rozproszonej EDS. Wyniki wykazują, że w badanym stopie zachodzi wyraźny podział na dwie ciecze. Mikrostruktura wlewka zawiera składnik eutektyczny bogaty w Fe, Si i B oraz fazę wzbogaconą w In.

Słowa kluczowe: kompozyt amorficzno-krystaliczny, kamera termowizyjna średniej podczerwieni, skaningowa mikroskopia elektronowa (SEM), termiczna analiza różnicowa (DTA)

Mirosława Wojciechowska M.Sc. Eng., Krzysztof Ziewiec Associate Professor Ph.D. Eng.: Pedagogical University of Cracow, Institute of Technology, Faculty of Mathematics, Physics and Technical Science, Krakow, Poland; **Jarosław Ferenc Ph.D. Eng.:** Warsaw University of Technology, Faculty of Materials Science and Engineering, Warsaw, Poland; mirwoj@up.krakow.pl

1. Introduction

Due to their useful physical, mechanical, and functional properties [1, 2], metallic glasses constitute a very promising group of materials; however researchers are still working on the preparation of glassy matrix composites mainly due to their poor ductility. One promising solution for this purpose is by the use of liquid immiscible systems [1, 3–6]. However, to utilize this feature in an optimal way, knowledge of the high-temperature characteristics of such alloys is necessary. One of the most-popular amorphous alloys is based on an Fe-Si-B system. On the other hand, it can be found that indium has low affinity to iron, silicon, and boron [7, 8]; therefore, one can anticipate that Fe-Si-B-In alloys provide good amorphization of the Fe-Si-B-rich constituents as well as liquid immiscibility of the In-rich constituent. The present work is devoted to an investigation of the high-temperature phase transformations and microstructure of Fe-Si-B-In alloys.

2. Experimental

The four-component $\text{Fe}_{71.25}\text{Si}_{9.5}\text{B}_{14.25}\text{In}_5$ alloy was prepared by arc melting starting with pure elements: 99.95 wt% Fe, 99.95 wt% Si, 99.95 wt% In, and an Fe-B ferroalloy in a protective atmosphere using Ti as a getter. Analysis of the microstructure and chemical composition of the ingot was performed using a JEOL 6610 scanning electron microscope with an Oxford X-ray microanalyzer. The 0.3 g ingot was remelted in the resistance furnace, and the alloy was observed during this remelting as well as during cooling using an MWIR FLIR SC7650 camera. The sample-to-camera distance was 150 mm, transmissivity of the window in the resistance furnace was 70 %, and the room temperature was 293 K. The areas for temperature measurement were selected in order to avoid the narcissus effect. The alloy was also investigated using a LABSYS DTA/DSC SETARAM differential scanning calorimeter at a heating rate of 40 K/min.

3. Results and discussion

The SEM microstructure of the $\text{Fe}_{71.25}\text{Si}_{9.5}\text{B}_{14.25}\text{In}_5$ alloy obtained from a cross-section of the resistance-melted ingot shown in Figure 1 is composed of two different regions. The darker component of the microstructure (Fig. 1a – left side) is predominantly composed of a fine eutectic constituent. The selected area of Fig. 1a marked by dashed-line rectangle is magnified below, and the black solid line indicates the EDS line scan (Fig. 1b). Figure 1b shows the concentration profiles for the alloying elements. This analysis shows that the bright areas of the SEM image are enriched in indium, while the dark areas are enriched in Fe and Si. It is expected that these areas are enriched in B [8]. There are also the Fe-rich spherulitic precipitates within the In-rich regions. This microstructure can be interpreted in terms of a high value of mixing enthalpy between

Fe and In (which is +19 kJ/mol [8]), because such a microstructure is typical for liquid-immiscible alloys [9–11]. The spherulitic morphology of the precipitates suggests that the particles found on both sides (Fe-rich and In-rich) were formed in a liquid state due to liquid miscibility occurring before crystallization.

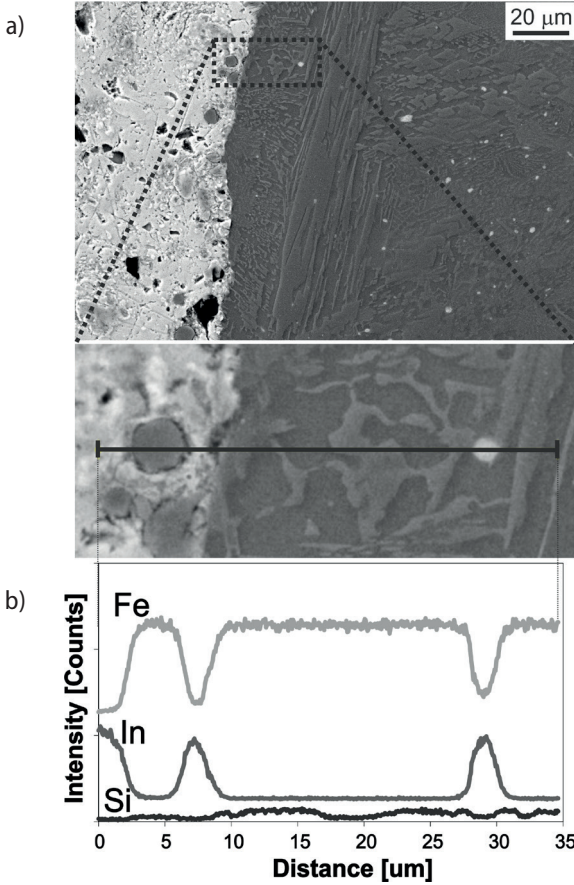


Fig. 1. Microstructure of $Fe_{71.25}Si_{9.5}B_{14.25}In_5$ ingot melted in resistance furnace: a) lower magnification (dotted rectangle is chosen for EDS line scan); b) EDS line scan of In, Fe, and Si

Figure 2 shows the results of IR (Infrared) observations of the $Fe_{71.25}Si_{9.5}B_{14.25}In_5$ alloy re-melted in the resistance furnace. The changes of apparent temperature and images of the sample for heating and cooling are shown in Figures 2a and 2b, respectively. The thin dashed lines marked on the diagrams correspond to the moment when the given image was captured. Both curves show a plateau where temperature arrests last ca. 4 seconds. The arrest upon heating occurs at 1540 K, and the corresponding value for cooling is at 1217 K. Assuming that the values of overheating and undercooling are equal, the

transformation temperature is 1378.5 K. It is worth mentioning that there were no the movements of the metal at the temperatures below 1540 K upon heating nor below 1217 K upon cooling. Furthermore, when continuous decrease of temperature is observed during cooling after the plateau (i.e., for 7.93 s and 12.08 s), there is a significant change in the sample appearance that can be attributed to the formation of an eutectic constituent. This suggests that the eutectic crystallization is a predominating mechanism of the sample crystallization. On the other hand, observation of all images of the liquid sample confirms that it had not reached a state of the homogeneous liquid, and two liquids were observed (Fig. 2c). This suggests that the miscibility gap occurs within the entire studied range of temperatures.

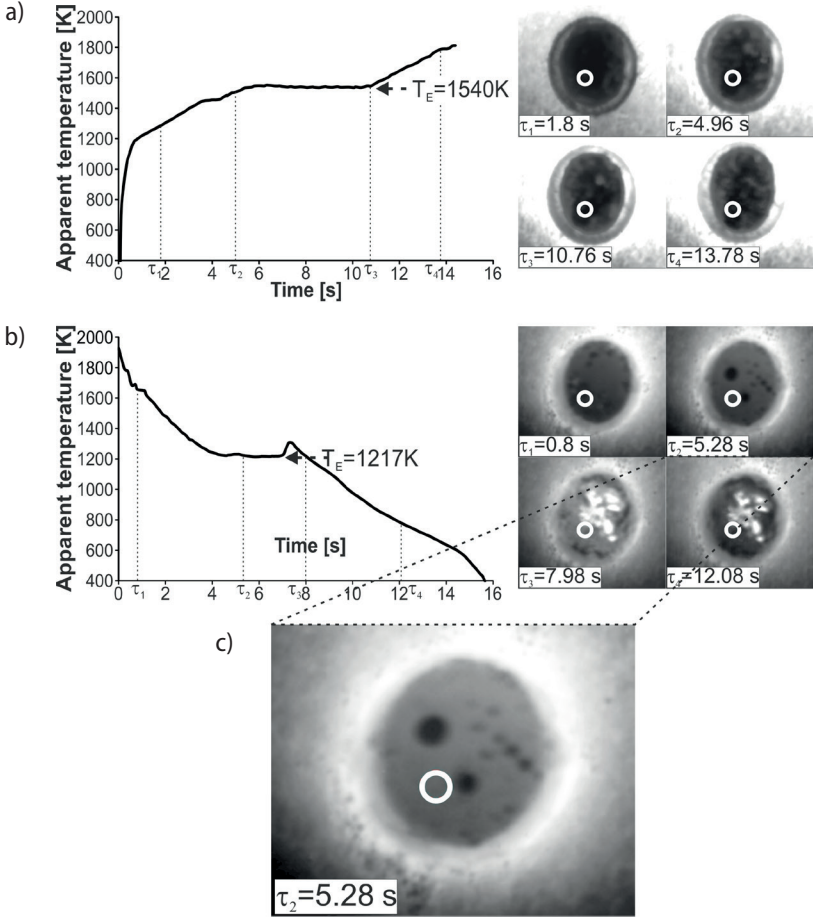


Fig. 2. IR-camera observations: a) changes of apparent temperature and images of the sample for heating; b) changes for cooling; c) magnified image of sample at $\tau_2 = 5.28\text{ s}$; white circles denote region of interest (ROI) for which temperature plots are presented

Figure 3 shows the DTA measurement for the heating and cooling of the $\text{Fe}_{71.25}\text{Si}_{9.5}\text{B}_{14.25}\text{In}_5$ alloy. The melting of the alloy probably starts at a low temperature when the melting point of the In-rich constituent is reached; however, it was not studied in the present work. Thus, melting of the remaining part of the alloy starts at $T_m = 1417$ K and ends at $T_l = 1481$ K. It is worth noting that, after the completion of melting at $T_l = 1481$ K, the DTA signal had not reached its level observed at $T_m = 1417$ K (shown by the dotted line – Fig. 3). On this basis (and referring to other works [11, 12]), it can be concluded that, in the present experiment, there is no mutual dissolution of the two immiscible liquids and a state of homogeneous liquid is not reached.

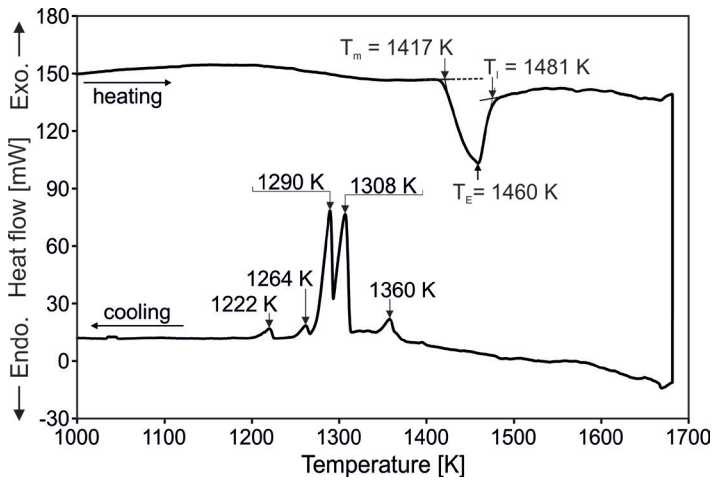


Fig. 3. DTA for heating and cooling at high temperature range

During the cooling five different peaks were recorded at 1360, 1308, 1290, 1264 and 1222 K. These exothermic peaks correspond to the crystallization of the liquid alloy. The presence of multiple peaks during crystallization was also observed in another work [11]. The alloys to which this effect applies present a miscibility gap: this suggests that it may be due to partitioning of the alloy into droplets of different chemical compositions, which results in the slightly different values of crystallization temperatures observed during DTA measurements.

4. Conclusions

- EDS analysis confirms our expectation about liquid phase partitioning, where the ingot microstructure presents very strong segregation into the eutectic regions enriched in the Fe-Si-B-rich and In-rich regions.

- The studied alloy presents a substantial thermal effect associated with eutectic transformation.
- There is no mutual dissolution of the two immiscible liquids nor their transformation into the homogeneous liquid within the studied temperature range (using both IR-imaging and DTA).
- The multiple peaks observed during crystallization may be due to partitioning of the alloy into droplets of different chemical compositions.

Acknowledgement

The study was financially supported by National Science Centre (NCN) (Project No. 2012/05/B/ST8/ 02644).

References

- [1] Warlimont H.: Amorphous metals driving materials and process innovations. *Materials Science and Engineering A*, 304–306 (2001), 61–67
- [2] Wang W.H.: Elastic moduli and behaviors of metallic glasses. *Journal of Non-Crystalline Solids*, 351 (2005), 1481–1485
- [3] Ashby M.F., Greer A.L.: Metallic glasses as structural materials. *Scripta Materialia*, 54 (2006), 321–326
- [4] Schäfer R.: Domains in ‘extremely’ soft magnetic materials. *Journal of Magnetism and Magnetic Materials*, 215–216 (2000), 652–663
- [5] Liaw P.K., Wang G., Schneider J.: Bulk metallic glasses: Overcoming the challenges to widespread applications. *Journal of The Metals & Materials Society*, 62, 2 (2010), 69
- [6] Kündig A.A., Ohnuma M., Ping D.H., Ohkubo T., Hono K.: In situ formed two-phase metallic glass with surface fractal microstructure. *Acta Materialia*, 52 (2004) 2441–2448
- [7] Boer F.R., Boom R., Mattens W.C.M., Miedema A.R., Niessen A.K.: *Cohesion in metals: transition metal alloys*, vol. 1. Elsevier Science, Amsterdam 1988
- [8] Takeuchi A., Inoue A.: Mixing enthalpy of liquid phase calculated by Miedema’s scheme and approximated with sub-regular solution model for assessing forming ability of amorphous and glassy alloys. *Intermetallics*, 18 (2010), 1779–1789
- [9] Ziewiec K.: Characterization of immiscible Ni₇₈Ag₂P₂₀ alloy and formation of amorphous/crystalline composite. *Journal of Non-Crystalline Solids*, 355 (2009), 2540–2543
- [10] Ziewiec K., Malczewski P., Boczkal G., Prusik K.: Formation and Properties of Amorphous/Crystalline Ductile Composites in Ni-Ag-P Immiscible Alloys. *Solid State Phenomena*, 186 (2012), 216–221
- [11] Ziewiec K., Wojciechowska M., Garzeł G., Czeppe T., Błachowski A., Ruebenbauer K.: Microstructure and phase transformations in a liquid immiscible Fe₆₀Cu₂₀P₁₀Si₅B₅ alloy. *Intermetallics*, 69 (2016), 47–53
- [12] Ratke L., Diefenbach S.: Liquid immiscible alloys. *Materials Science and Engineering R: Reports*, 15, 7–8 (1995), 263–347